Proceedings of the

Advanced Architectures in Photonics

September 21–24, 2014
Prague, Czech Republic

Volume 1

Editors

Jiri Orava

University of Cambridge
Department of Materials Science and Metallurgy
27 Charles Babbage Road
CB3 0FS Cambridge
United Kingdom

Tohoku University
WPI-Advanced Institute for Materials Research
(WPI-AIMR)
2-1-1 Katahira, Aoba-ku
980-8577 Sendai
Japan

Tomas Kohoutek

Involved Ltd.
Siroka 1
537 01 Chrudim
Czech Republic

Proceeding of the Advanced Architectures in Photonics
http://aap-conference.com/aap-proceedings

ISSN: 2336-6036
September 2014

Published by **Involved Ltd.**
Address: Siroka 1, 53701, Chrudim, Czech Republic
Email: info@involved.cz, Tel. +420 732 974 096

CONTENTS

Proceedings of the Advanced Architectures in Photonics 1, 15–18 (2014)

Stimuli-responsive colloidal crystal films

C. G. Schäfer,* S. Heidt, D. Scheid and M. Gallei

Ernst-Berl Institute for Chemical Engineering and Macromolecular Science, Technische Universität Darmstadt, Alarich-Weiss-Straße 4, D-64287 Darmstadt, Germany

*Electronic mail: c.schaefer@mc.tu-darmstadt.de

In this contribution, the preparation of highly thermo-responsive colloidal crystal films featuring switchable structural colour is reported. Novel organic/inorganic hybrid core-interlayer-shell (CIS) architectures based on silica core particles and poly(*N*-isopropylacrylamide-*co*-methyl methacrylate) (P(NIPAM-*co*-MMA)) as shell polymer are synthesised via multi-step synthetic protocols. The use of PNIPAM as comonomer for shell growth leads to highly monodisperse CIS particles containing a film-forming shell, which additionally provides temperature-responsive swelling and deswelling in water. Directed self-assembly of the hybrid CIS particles using feasible melt-shear organization and subsequent UV crosslinking leads to mechanically stable and well-ordered colloidal crystal films. Thermo-responsive structural colour change of these novel films is found to be repeatedly addressable. We expect herein described strategies for the preparation of responsive colloidal architectures in combination with the powerful melt-shear organization technique opens access to novel large-scalable stimuli-responsive colloidal crystal films which are expected to be promising candidates for a wide range of optical sensing applications.

Photonic crystals have attracted a great deal of attention as potential candidates for next generation optoelectronic applications due to their intrinsic capability to manipulate and control the propagation of light in a certain frequency range [1]. Such materials reveal a periodic modulation of the refractive index on the length scale of the wavelength of light, which leads to the appearance of forbidden regions for photons in the photonic band structure (photonic bandgaps). Examples of such materials can be found in nature, such as the morpho butterflies, the Japanese jewel beetles and natural opal gemstones [2]. Artificially, functional photonic crystals can be created by assembling monodisperse colloidal particles into periodically ordered structures, also referred to as *colloidal crystals*. At micro scales such colloidal crystals are composed of monodisperse spheres from 150 to 350 nm in diameter arranged in a face centered cubic (fcc) lattice. As the distance between the packed planes of spheres is on the length scale of visible light, light of a certain wavelength is reflected corresponding to Bragg's law. In the recent past several techniques were developed and optimized to build up such fascinating structures from simple spheres of various materials [3–5]. However, the optical properties of such materials strongly depend on the degree of crystallinity and the refractive index contrast between the spheres and the surrounding material. To a first approximation it is expected that the reflected colour varies as a function of the incident angle. Therefore, brilliant angle-dependent reflection colours can be observed only by tilting the particle-based photonic material. Over the last decade so-called *elastomeric colloidal crystal films* attracted a great deal of attention due to their reversible structural colour change upon mechanically induced deformation, *i.e.*, simply by stretching the entire film.[5-9] These mechanochromic materials are interesting candidates for sensing devices and actuation systems. On the other hand various external triggers, such as ions [10], pH [11], solvents [11,12], redox reagents [13], electric or magnetic fields can additionally be used in order to change the lattice structure and thus the structural colour [14–15]. Especially the incorporation of thermo-responsive polymers is unambiguously attractive as responsiveness can be considered to be relatively fast, fully reversible and non-invasive [16–19].

Within the herein presented approach, the melt-shear organization technique is combined with complex stimuli-responsive hybrid particle architectures. A facile strategy for the preparation of novel large-scalable organic/inorganic hybrid colloidal crystal films featuring a fully reversible thermochromic response is reported. For this purpose, highly monodisperse core-interlayer-shell (CIS) particles consisting of an inorganic silica core, an organic poly(methyl methacrylate) (PMMA) interlayer and an organic poly(*N*-isopropylacrylamide-*co*-methyl methacrylate) (P(NIPAM-*co*-MMA)) shell (silica@PMMA@P(NIPAM-*co*-MMA)) are synthesized following a multi-step synthetic protocol. By taking advantage of P(NIPAM-*co*-MMA) as shell material, these monodisperse particles reveal an excellent temperature-responsive behaviour accompanied with a temperature-induced volume phase transition in water. By applying the feasible melt-shear organization technique to the CIS particles, highly ordered colloidal crystal structures showing remarkably distinct and iridescent reflection colours are obtained. Subsequent UV crosslinking strategies lead to fully reversible thermo-responsive colloidal crystal films, which can be utilized for optical sensor applications.

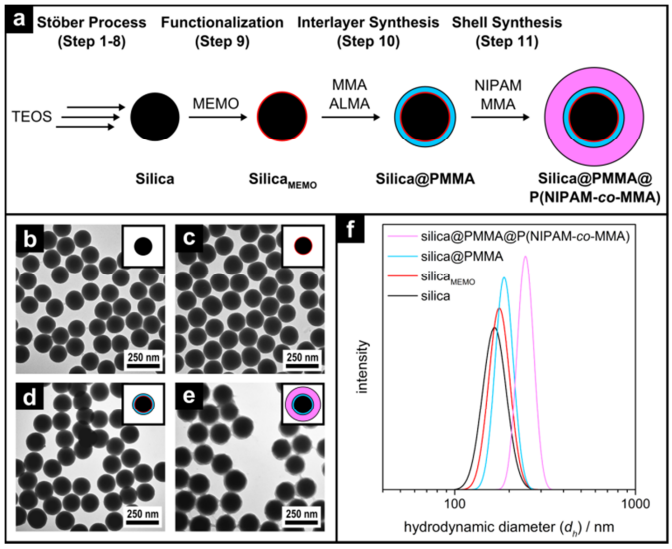

Figure 1. (a) Scheme of the stepwise synthesis of silica@PMMA@P(NIPAM-*co*-MMA) CIS particles. (b-e) TEM images of particles after different synthetic steps (scale bars correspond to 250 nm). (c) DLS measurements of corresponding particles.

The precursor material consisting of silica@PMMA@P(NIPAM-*co*-MMA) CIS particles was prepared using a multi-step synthetic protocol leading to particles featuring narrowly distributed particle diameters, as depicted in Fig. 1a.

First, silica core particles were synthesized according to a modified Stöber process, starting from silica seed particles that were prepared by the hydrolysis and condensation of tetraethoxysilane (TEOS) in ethanol (Step 1) [20]. The silica seeds were further increased in size over several consecutive growing steps by the stepwise addition of TEOS (Step 2–8). The size of the silica core particles could easily be adjusted by the number of these growing steps. Afterwards the surface of silica cores was functionalization with 3-methacryloxypropyltrimethoxysilane (MEMO) (Step 9), which generates a hydrophobic surface on the silica particles and in addition can afterwards react in the radical polymerization allowing for grafting the polymer shell onto the silica cores. For subsequent emulsion polymerization, ethanol was removed by distillation and completely substituted by water without isolating the particles. In the next steps semicontinuous and stepwise emulsion polymerization protocols in the presence of functionalized silica cores (silica$_{MEMO}$) were applied in order to produce silica/polymer hybrid CIS particles. A PMMA interlayer was formed that was slightly crosslinked by using allyl methacrylate (ALMA) as comonomer (silica@PMMA, Step 10). Noteworthy, ALMA served as a grafting anchor for the final shell chains and the PNIPAM-containing shell grew better on PMMA than

Table I. Comparison of Average Particle Diameters Determined by TEM and DLS Measurements.

sample	d_{TEM} [a] [nm]	d_{DLS} [b] [nm]
silica	154 ± 3	160 ± 25
$silica_{MEMO}$	161 ± 5	172 ± 22
silica@PMMA	170 ± 7	185 ± 20
silica@PMMA@ P(NIPAM-*co*-MMA)	188 ± 8	248 ± 23

[a] Average sphere diameter and standard deviation determined by counting at least 100 particles out of the TEM images; [b] Average sphere diameter and standard deviation determined at the maximum of the logarithmic probability density of the particle size distribution.

on functionalized $silica_{MEMO}$ cores. We note that a proper core-shell connection is crucial for the entire particle stability while applying the melt-shear organization technique [5–7,12,13,19]. Finally, NIPAM and MMA were added to obtain a film-forming PNIPAM-containing gel shell (silica@PMMA@P(NIPAM-*co*-MMA), Step 11). The successful build-up of the internal CIS particle architecture was characterized by transmission electron microscopy (TEM). Fig. 1 shows respective TEM images of the particles after key steps of the particle synthesis, verifying that monodisperse and spherical silica cores (Fig. 1b), separated functionalized $silica_{MEMO}$ particles (Fig. 1c), silica@PMMA core-interlayer particles (Fig. 1d) and finally silica@PMMA@P(NIPAM-*co*-MMA) CIS particles (Fig. 1e) were formed. Inevitably, particle coalescence occurred when the final CIS particles were dried on the supporting grid for TEM measurements, but a P(NIPAM-*co*-MMA) gel shell was still clearly visible in the corresponding TEM images. In addition to TEM investigations, hydrodynamic diameters and size distributions of the particles after the different synthetic steps were characterized by using dynamic light scattering (DLS, Fig. 1f). The average diameters obtained by TEM (d_{TEM}) and hydrodynamic diameters obtained by DLS measurements (d_{DLS}) are summarized in Tab. I and were in excellent agreement with expectations.

In order to investigate the thermo-responsiveness of herein prepared novel hybrid CIS particles, the swelling and shrinking behaviour of P(NIPAM-*co*-MMA) shell in water was studied by using temperature-dependent DLS measurements. To demonstrate the temperature-induced volume phase transition of surface-anchored polymers, the particle dispersion was repeatedly brought above or below the LCST of PNIPAM (~ 32°C). In detail, the particles were first cooled from 40.0°C to 15.0°C and again heated up to 40.0°C. Fig. 2a shows the hydrodynamic diameter (d_h) of the particles as a function of temperature for the first cooling run.

As expected, the DLS results show a tremendous increase of d_h with a decrease in temperature from initial 217 nm at 40.0°C to 364 nm after cooling to 15.0°C, which corresponds to a distinct volume phase transition of the P(NIPAM-*co*-MMA) shell polymer (Fig. 2a). The shell thickness varied most significant while approaching the LCST of PNIPAM, while only minor changes were observed above the LCST (*cf.* in the temperature range from 40°C to 35°C). These results point out that the hydrophobic MMA comonomer did not significantly affect the thermo-responsive behaviour of PNIPAM. Moreover, it evidenced the possibility to manipulate the optical properties of corresponding PNIPAM-containing colloidal crystal gel films simply by changing the temperature above or below the LCST of PNIPAM. Noteworthy, in the case of the pristine CIS particle dispersion prior to the preparation of colloidal crystal films, the shells were not crosslinked. Hence, after several cooling-heating cycles the outer part of the polymer shell tended to peel off since only the inner polymer chains were grafted to the interlayer. Therefore no fully reversible thermo-responsive behaviour of the CIS particles could be achieved. Compared to these results found for the particle dispersion, obstacles proving the full reversibility can be circumvented by an *a posteriori* crosslinking approach in the colloidal crystal films which will be described in the ensuing section.

Based on these novel thermo-responsive silica@PMMA@P(NIPAM-*co*-MMA) CIS particles, colloidal crystal films were prepared by applying the melt-shear organization technique. A scheme of the preparation process is depicted in Fig. 3a.

Particles were separated from their dispersion by coagulation and drying. After complete removal of the dispersion medium, the particles

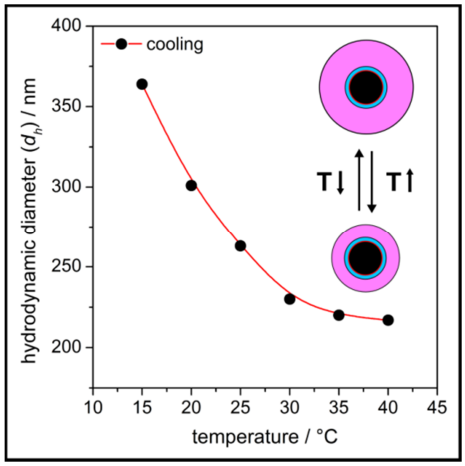

Figure 2. Temperature-dependent DLS investigations of silica@PMMA@P(NIPAM-*co*-MMA) particle dispersion in water, accompanied by a volume phase transition of the P(NIPAM-*co*-MMA) shell (the red solid line is a guide for the eye only).

featured the consistency of a hard solid at room temperature due to the relatively high glass transition temperature (Tg) of P(NIPAM-*co*-MMA) copolymer (Tg ~ 120°C). At elevated temperature the shell polymer of the hard CIS particles was capable to merge into a viscous liquid forming a continuous molten matrix. Therefore, the particle precursor powder could be mixed with different crosslinking agents (*e.g.,* bifunctional monomer *N*,*N*'-(1,2-dihydroxyethylene) bisacrylamide (DHEBA), UV initiators benzophenone and Irgacure 184, ratio = 88:10:1:1 by weight) by using extrusion, whereby the different components formed homogeneous mixtures. For colloidal crystal film preparation, the mixture was heated between the plates of a laboratory press and melt flow was induced by applying pressure perpendicular to the plates. Under these conditions, the melt flowed sideways in a parabolic flow field profile in which the particles crystallized. As result, a precise fcc arrangement of stacked hexagonal layers of hard silica cores embedded in the P(NIPAM-*co*-MMA) matrix can thus be obtained. The (111) planes of the fcc lattice were parallel aligned to the prepared film surfaces. After melt-shear organization the formation of a mechanically stable colloidal crystal film was achieved by subsequent crosslinking reactions (xlink) of the matrix polymer. During UV irradiation, the free polymer chains in the P(NIPAM-*co*-MMA) matrix were linked with embedded DHEBA monomer generating a dense crosslink network. As can be concluded from the corresponding image (Fig. 3b), the resultant colloidal crystal film revealed a brilliant and distinct purple iridescent reflection colour. The precise arrangement of the surface parallel (111) planes was proven by scanning electron microscopy (SEM) investigations of the corresponding film surface. After etching the matrix material with oxygen plasma, hexagonally arranged silica cores (light) became visible in the corresponding SEM image (Fig. 3c). Out of Fig. 3 it can be concluded, that the melt-shear organization of herein investigated novel PNIPAM-containing hybrid CIS particles led to an almost perfectly ordered colloidal crystalline structure. The subsequent crosslinking reaction of the matrix polymer provided stable and solid films, which is the basic prerequisite for a homogeneous temperature-induced swelling and deswelling and hence a fully reversible tuning of the structural colour.

In the following, the optical response of the prepared colloidal crystal film was investigated with regard to its thermochromic behaviour and its usability for optical temperature sensing applications. For the determination of temperature-induced structural colour shifts, the PNIPAM-containing film was first swollen in water, which led to the formation of a photonic hydrogel film. Afterwards, the film was cooled from T = 20°C down to 0.5°C. We note that the transition temperature shifted to lower temperatures (< 20°C) compared to the LCST found for the purified single particle dispersion (see Fig. 2), due to the presence of a high amount of different crosslinking additives (*e.g.*, benzophenone, Irgacure 184 and DHEBA). The temperature-induced swelling and deswelling phenomena of the colloidal crystal structure as well as corresponding UV-vis reflection measurements are shown in Fig. 4.

The original colloidal crystal film was capable of slight swelling in water already at 20°C forming a photonic hydrogel film and changing the original purple reflection colour (Fig. 3b) to green (Fig 4b). The stopband which corresponds to the (111)-lattice planes generated a Bragg peak whose spectral position in the visible region corresponds to the plane spacing of stacks of the hexagonally arranged silica cores

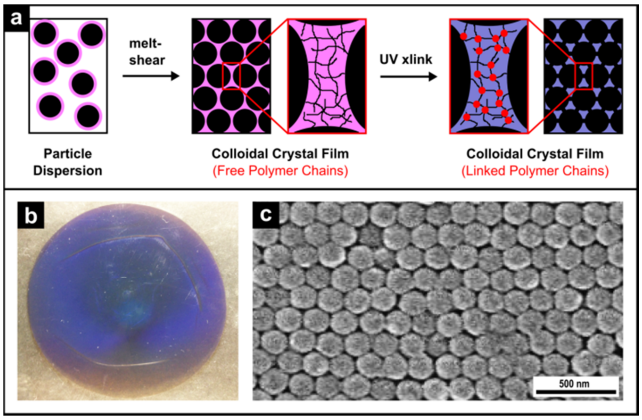

Figure 3. a) Scheme of the processing of silica@PMMA@P(NIPAM-*co*-MMA) CIS particles into highly-ordered and crosslinked (xlink) colloidal crystal films. (b) Photograph of prepared film showing the brilliant and distinct purple iridescent reflection colour. (c) SEM image of oxygen plasma-etched surface of the colloidal crystal film showing the hexagonally arranged (111) plane of silica spheres.

embedded in the PNIPAM-containing matrix. The wavelength of the reflected colour of the colloidal crystal gel can be well described by combining Bragg's law with Snell's law (Eq. 1):

$$\lambda_{111} = 2\, a_{111}\, (n_{eff}^{\,2} - \sin^2\theta)^{1/2}, \qquad (1)$$

where a_{111} denotes the lattice spacing of the (111) plane and θ the angle of incident light. The average refractive index n_{eff} can be calculated by considering the indices (n_i) and the volume fractions (ϕ_i) of the silica cores and the polymer shells as well as the water content of the gel under certain conditions according to Eq. 2:

$$n_{eff} = \sum n_i\, \phi_i. \qquad (2)$$

According to Eq. 1, temperature-responsiveness of colloidal crystal gels mainly depends on temperature-induced volume phase transition (q) from $q = 0$ to $q = q^*$ accompanied with changes in the (111) lattice plane spacing (a_{111}) from a_{111} to a_{q^*} as illustrated in Fig. 4a. In addition, it is well known that the intensity of the reflection peaks is proportional to both the magnitude of the refractive index contrast and the number of ordered lattice planes that result from the periodic fcc arrangement. Fig. 4b shows the temperature-dependent reflection spectra for the PNIPAM-containing colloidal crystal gel as well as the observed changes in reflection colour, which evidence a temperature-induced swelling while passing the LCST of the PNIPAM-containing matrix. As expected, the volume phase transition was accompanied by a stopband shift of almost 150 nm, *i.e.*, a change from green (λ = 551 nm) to red (λ = 698 nm) of the Bragg peak under normal light incidence (θ = 90°). Three general spectral characteristics of the colloidal crystal film have to be noted as the temperature decreased: first, the peak shifted toward larger wavelengths indicating an increase of the (111) lattice plane spacing; second, the intensity of the peak increased until reaching 5.0°C due to an increase in refractive index contrast since the volume fraction of water featuring a comparably lower refractive index was increased in the matrix material; third, the increase in peak width that arose at the half maximum of the peaks upon the abrupt volume change as well as the decrease in peak intensity from 5.0°C to 0.5°C, which is a sign of a certain loss of order in the colloidal crystalline structure. The distortion may be induced by differences in lattice plane spacing over the entire thickness of the gel film. However, a remarkable order of the particle structure was still present since the diffraction peak was clearly visible. In addition, the temperature response was found to be fully reversible over at least two cooling-heating cycles with good reproducibility (variations in λ_{max} of ± 10 nm) induced by rapidly switching the temperature between 0.5°C and 20.0°C (Fig. 4c). Due to matrix polymer crosslinking the original colloidal crystal structure with nearly identical lattice plane spacing and order was totally restored after temperature-induced deswelling.

In summary, a convenient synthetic strategy for the preparation of novel thermo-responsive silica@PMMA@P(NIPAM-*co*-MMA) CIS architectures was reported. The powerful melt-shear organization technique and application of crosslinking protocols were utilized to prepare large-scaled colloidal crystal films. Corresponding photonic

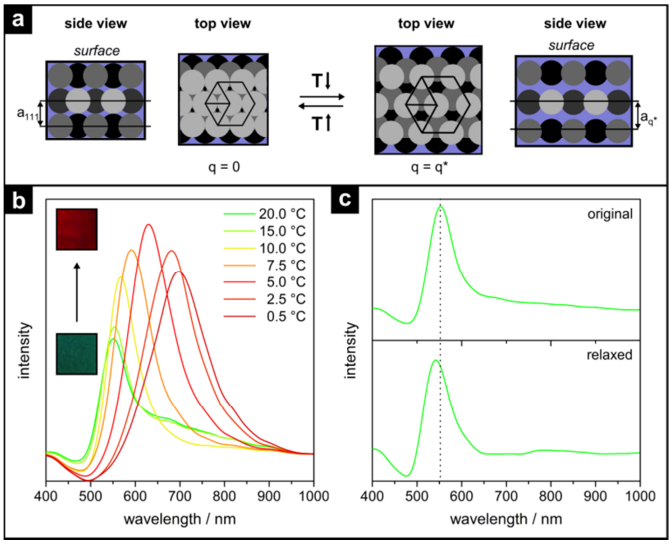

Figure 4. (a) Scheme showing the reversible temperature (T)-induced volume phase transition (q) of the colloidal crystal lattice of silica core particles (grey to black) embedded in the P(NIPAM-*co*-MMA) matrix (purple), accompanied by a change in the (111) lattice plane spacing (a_{111}). (b) UV-vis reflection spectra of swollen colloidal crystal gel film showing the temperature-induced shifts of the Bragg wavelength (λ_{111}) (insets: photographs of swollen photonic hydrogel film before and after temperature-induced colour tuning). (c) Comparison of reflection spectra of the original gel film and the relaxed gel film after cooling to 0.5°C and subsequent heating to 20°C.

gels showed an excellent reversible thermo-responsive behaviour accompanied with reversible tunable structural colour. We expect herein investigated PNIPAM-containing soft photonic materials featuring a remarkable thermo-responsive character as promising candidates for optical sensor devices and reversibly switchable photonic bandgap materials.

MATERIALS AND METHODS

TEM was performed on a Zeiss EM10 at an operating voltage of 60 kV. SEM was performed on a Philips XL30 FEG at an operating voltage of 20 kV. For DLS measurements of the particle dispersions a Nanophox photon cross-correlation spectrometer (Sympatec) was used. The experiments were carried out at an angle of 90° at 20°C. The temperature-dependent DLS experiments were performed in the temperature range from 40.0°C to 15.0°C using the same setup. Reflection spectra were recorded using a vis-NIR fiber spectrophotometer (USB 2000, Ocean Optics). For the reflection measurements a deuterium/tungsten halogen lamp (DT mini 2, Ocean Optics) was used.

All chemicals were purchased from VWR and Sigma Aldrich and used as received if not otherwise mentioned. Prior to use in the emulsion polymerization, the stabilizers hydroquinone monomethylether was removed from MMA monomer. For this purpose, MMA was extracted with 1 M sodium hydroxide solution, washed with water until the solution was neutral followed by drying over sodium sulfate.

Silica particle dispersions in ethanol with a final SiO_2 solid content of 2.5 wt% were prepared following the procedure described by van Blaaderen *et al.* [20] 1240 mL of this ethanolic dispersion was mixed with 1.53 mL MEMO, diluted with 6 ml ethanol. The mixture was slowly heated to 60°C and stirred for 1 h and ammonia was removed under reduced pressure. Then the water was removed by azeotropic distillation of the ethanol/water mixture at 60°C, while the volume was kept constant by continuous addition of ethanol. When the dispersion was free of water, the volume was reduced to 350 mL and stirring was continued for additional 90 min at 60°C. To transfer the particles into an aqueous dispersion medium, a solution of 50 mg sodiumdodecylsulfate (SDS) in 100 g of water was added and ethanol was removed by azeotropic distillation, while the volume was kept constant by continuous addition of water. When the dispersion was free of ethanol, the volume was reduced to 200 ml. The final $silica_{MEMO}$ dispersion had a solid content of 15.6 wt.%.

Under argon, a 250 mL flask equipped with stirrer and reflux condenser was filled at 75 °C with 140 g of $silica_{MEMO}$ particle dispersion and a solution of 60 mg SDS in 10 g water was added. The polymerization was initiated immediately by adding 50 mg sodium peroxodisulfate (SPS). After 10 min, a monomer emulsion containing 0.2 g ALMA, 1.05 g MMA, 0.35 g Dowfax 2A1, 0.4 g KOH and 15 g water was added continuously over a period of 1 h (silica@PMMA). After 15 min of reaction time, 10 mg SPS were added. After additional 10 min, a monomer emulsion of 5.9 g NIPAM, 5.9 g MMA 0.37 g SDS and 22.0 g water was added continuously over a period of 1.8 h (silica@PMMA@P(NIPAM-*co*-MMA) shell). After additional 60 min, the product is cooled to room temperature.

For preparation of colloidal crystal films, the latex was dried at 40°C. The precursor powder was mixed with 0.05 wt% of carbon-black (Special Black 4, Degussa), 1 wt% benzophenone, 1 wt% Irgacure 184 and 10 wt% DHEBA in a microextruder (micro1, DSM Research) at 180°C. A 1 g portion of the mixture was covered with PET film and heated to 180°C between the plates of a

laboratory press (300E, Dr. Collin). Melt flow was induced by applying a pressure of 150 bar for 3 min, resulting in a colloidal crystal film of about 10 cm in diameter. For subsequent crosslinking, the film was irradiated with an industrial-type mercury lamp (UV Cube 2000, Dr. Hoenle) with an output power of 1000 W. The PET-covered films were treated at a distance of 10 cm for 2 min from both sides.

ACKNOWLEDGEMENT
The authors thank Christina Lederle (department of physics, TU Darmstadt) for help with DLS measurements. The authors acknowledge the Landesoffensive zur Entwicklung Wissenschaftlisch-Ökonomischer Exzellenz (LOEWE) of the State of Hesse through research initiative Soft Control for ongoing financial support. C. G. S. thanks the Vereinigung von Freunden der Technischen Universität zu Darmstadt e.V. and the Klein, Schanzlin & Becker (KSB)-Stiftung for financial support.

REFERENCES

[1] J. D. Joannopoulos, S. G. Johnson, J. N. Winn, R. D. Meade, *Photonic crystals: Molding the flow of light*, 2nd ed. Princeton University Press, New Jersey, 2008.

[2] S. Kinoshita, S. Yoshioka, Structural colors in nature: The role of regularity and irregularity in the structure, *ChemPhysChem* **6**, 1442–1459 (2005).

[3] J. F. Galisteo-López, M. Ibisate, R. Sapienza, L. S. Froufe-Pérez, Á. Blanco, C. López, Self-assembled photonic structures, *Adv. Mater.* **23**, 30–69 (2011).

[4] F. Li, D. P. Josephson, A. Stein, Colloidal Assembly, The toad from particles to colloidal molecules and crystals, *Angew. Chem. Int. Ed.* **50**, 360–388 (2011).

[5] C. G. Schäfer, M. Gallei, J. T. Zahn, J. Engelhardt, G. P. Hellmann, M. Rehahn, Reversible light-, thermo-, and mechano-responsive elastomeric polymer opal films, *Chem. Mater.* **25**, 2309–2318 (2013).

[6] C. G. Schäfer, D. A. Smolin, G. P. Hellmann, M. Gallei, Fully reversible shape transition of soft spheres in elastomeric polymer opal films, *Langmuir* **29**, 11275–11283 (2013).

[7] C. G. Schäfer, B. Viel, G. P. Hellmann, M. Rehahn, M. Gallei, Thermo-cross-linked elastomeric opal films, *ACS Appl. Mater. Interfaces* **5**, 10623–10632 (2013).

[8] H. Fudouzi, T. Sawada, Photonic rubber sheets with tunable color by elastic deformation, *Langmuir* **22**, 1365–1368 (2006).

[9] D. Yang, S. Ye, J. Ge, From metastable colloidal crystalline arrays to fast responsive mechanochromic photonic gels: An organic gel for deformation-based display panels, *Adv. Opt. Mater.* **24**, 3197–3205 (2014).

[10] J. H. Holtz, S. A. Asher, Polymerized colloidal crystal hydrogel films as intelligent chemical sensing materials, *Nature* **389**, 829–832 (1997).

[11] X. Xu, A. V. Goponenko, S. A. Asher, Polymerized polyHEMA photonic crystals: pH and ethanol sensor materials, *J. Am. Chem. Soc.* **130**, 3113–3119 (2008).

[12] C. G. Schäfer, M. Biesalski, G. P. Hellmann, M. Rehahn, M. Gallei, Paper-supported elastomeric opal films for enhanced and reversible solvatochromic response, *J. Nanophoton.* **7**, 070599–070599 (2013).

[13] D. Scheid, C. Lederle, S. Vowinkel, C. G. Schäfer, B. Stühn, M. Gallei, Redox-and mechano-chromic response of metallopolymer-based elastomeric colloidal crystal films, *J. Mater. Chem. C* **2**, 2583–2590 (2014).

[14] A. C. Arsenault, D. P. Puzzo, I. Manners, G. A. Ozin, Photonic-crystal full-colour displays, *Nature Photonics* **1**, 468–472 (2007).

[15] J. Ge, Y. Yin, Magnetically responsive colloidal photonic crystals, *J. Mater. Chem.* **18**, 5041–5045 (2008).

[16] Y. Takeoka, M. Watanabe, Template synthesis and optical properties of chameleonic poly(*N*-isopropylacrylamide) gels using closest-packed self-assembled colloidal silica crystals, *Adv. Mater.* **15**, 199–201 (2003).

[17] C. E. Reese, A. V. Mikhonin, M. Kamenjicki, A. Tikhonov, S. A. Asher, Nanogel nanosecond photonic crystal optical switching, *J. Am. Chem. Soc.* **126**, 1493–1496 (2004).

[18] A. Espinha, M. Concepción Serrano, A. Blanco, C. López, Thermoresponsive shape-memory photonic nanostructures, *Adv. Opt. Mater.* **2**, 516–521 (2014).

[19] C. G. Schäfer, C. Lederle, K. Zentel, B. Stühn, M. Gallei, Utilising stretch-tunable thermochromic elastomeric opal films as novel reversible switchable photonic materials, *Macromol. Rapid Commun.* **35**,1852–1860 (2014) .

[20] C. Graf, A. van Blaaderen, Metallodielectric colloidal core-shell particles for photonic applications, *Langmuir* **18**, 524–534 (2002).